Supporting information for

In vivo Biodistribution of Kinetically Stable Pt_2L_4 Nanospheres that Show Anti-Cancer Activity

Eduard O. Bobylev[a+], Renzo A. Knol[b+], Simon Mathew[a], David A. Poole III[a], Ioli Kotsogianni[c], Nathaniel I. Martin[c], Bas de Bruin[a], Alexander Kros[b*], Joost N.H. Reek[a*]

[a] van 't Hoff Institute for Molecular Sciences, University of Amsterdam, Science Park 904, 1098 XH Amsterdam, the Netherlands.

[b] Dept. of Supramolecular & Biomaterials Chemistry, Leiden Institute of Chemistry, Leiden University, P.O. Box 9502, 2300 RA, Leiden, The Netherlands.

[c] Biological Chemistry Group, Institute of Biology Leiden, Leiden University 2333 BE Leiden, The Netherlands.

[+] These authors contributed equally to this work.

List of content:

Materials and methods

General procedures: All synthetic procedures were carried out under a nitrogen atmosphere using standard Schlenk techniques. All commercially available chemicals were used as received without further purification. Solvents used for synthesis were dried, distilled and degassed with the most suitable method. Column chromatography was performed open to air using solvents as received.

Cryospray-ionization MS (CSI–MS): Mass spectra were collected on a HR–ToF Bruker Daltonik GmbH (Bremen, Germany) Impact II, an ESI–ToF–MS capable of resolution of at least 40000 FWHM, which was coupled to a Bruker cryospray unit. Detection was in positive-ion mode and the source voltage was between 4 and 6 kV. The sample was introduced with a syringe pump at a flow rate of 18 ul hr^{-1}. The drying gas (N_2) was held at 40°C and the spray gas was held at 60°C. The machine was calibrated prior to every experiment via direct infusion of a TFA-Na solution, which provided a *m/z* range of singly charged peaks up to 3500 Da in both ion modes. Software acquisition Compass 2.0 for Otof series. Software processing m- mass.

UV–VIS: Measurements were performed on a Shimadzu UV-2600, 240V IVDD UV–VIS spectrophotometer.

UV–Vis stability: UV–Vis absorbance spectra were measured at 37°C, from 200 to 800 nm. Overnight spectra for the stability testing were collected with Scan Speed Medium 0.5, Scan Mode Repeat, 84 repetitions and a time interval of 600 s. UV–Vis spectrum of spheres in 3 mL PBS buffer (1 M, pH 7.4) were measured overnight and are displayed in the main text.

NMR stability: NMR data were obtained using a Bruker AV300, AV400, AV500 or AV300II spectrometer by measuring every 10 minutes for 14 hours at 37°C. A general procedure for the ^{1}H-NMR stability testing was used for the spheres as follows: To a vial containing 200 µL sphere in CD_3CN (2.5 mM, 0.5 µmol, 1 eq.), imidazole (0.7 mg, 10 µmol, 20 eq.) in D_2O (311 µL) was added. This was followed by glutathione (6.1 mg, 20 µmol, 40 eq.) and sodium chloride (1.74 mg, 30 µmol, 60 eq.) in D_2O (89 µL). ^{1}H-NMR was taken overnight.

Fluorescence and quantum yield: Spectra were recorded on a Fluorolog Jobin Yvon-SPEX together with their corresponding UV–Vis spectra (Shimadzu UV-2700 Spectrometer). The quantum yields were determined by a calibration of specific machine settings using rhodamine B as a standard. The obtained calibration curve (from three datapoints) displayed good agreement with a second standard probe (rhodamine 6G, error of QY determination ± 10%).

In vitro studies: Cells of the cancer cell lines PCM3-Pro4 (human prostate cancer) and MDA-MB-231 (human breast cancer) were selected based on expected susceptibility to anticancer activity of Pt metallaspheres in previous literature[1]. The cells were seeded in 96-well microplates DMEM high glucose (Sigma) supplemented with FCS (10%) and sodium pyruvate (1 mM) at 10^5 cells per well and incubated at 37˚C, 5% CO_2, for 24 hours. The medium was removed and fresh medium containing the samples (spheres, BBs, dummy's, Pt precursor) at the highest tested concentration was prepared and 100 µl added to each well in triplicates following a serial dilution with fresh medium to the lowest tested concentration. As a control, fresh medium containing DMSO to the same final concentration as in the samples was tested. The cells were incubated for 24 hours at 37˚C, 5% CO_2. Then 9 µl WST-1 reagent (Sigma) was added to each well mixed, and incubated for 2 hours at 37˚C, 5% CO_2. Then the absorbance at 400 nm was measured for each well, using the Infinite M1000Pro plate reader (Tecan).

ITC: A pilot was performed using 12.5 mM stock of $Pt_2L^{TEGRB}{}_4$ diluted to a final concentration of 40 µM in 10 mM HEPES (pH = 7.2) and BSA to a final concentration of 400 µM in 10 mM HEPES. The experiment was carried out at 25 ˚C. Although binding was observed, it was concluded that the ratio between the solutions should be around 1:7 instead of 1:10 and the concentrations should be a bit higher to obtain better results. Then, the 2.5 mM stock solutions of $Pt_2L^{RB}{}_4$ and $Pt_2L^{TEGRB}{}_4$ were heated for 30 minutes at 80 ˚C. The heated stocks were diluted in 10 mM HEPES to a final concentration of 100 µM (final DMSO concentration 4%). BSA was dissolved in 10 mM HEPES (exactly the same buffer) and diluted to a final concentration of 700 µM. The BSA solution being more viscous, was selected to load into the syringe to be injected into the wells containing the sphere solutions. The BSA solution was injected 25 times into the sphere solutions, as well as 10 mM HEPES without sphere as a control, and the resulting heat transfer was measured using microcalorimeter MicroCal PEAQ-ITC (Malvern). The experiment was carried out at 28 ˚C (the same temperature in which zebrafish embryos are incubated).

In vivo studies: The spheres were heated at 80 ˚C for 30-60 min, diluted in 10 mM HEPES or 1x PBS (pH 7.4) and then directly 1 nanoliter injected intravenously into the duct of Cuvier in 48–80 hours post fertilisation (hpf) zebrafish embryos using a capillary needle and Eppendorf FemtoJet injection setup. BSA samples were prepared in advance and injected diluted in buffer. Either the *kdrl*:GFP transgenic zebrafish line (http://zfin.org/ZDB-TGCONSTRCT-070529-1#summary GFP labeled vasculature) or *mpeg*:GFP transgenic zebrafish line (macrophages GFP labeled) was used at 48–80 hours post fertilisation (hpf). The biodistribution of the particles was analysed using the Leica SP8 confocal microscope by taking pictures at the time as indicated in the file name (30- or 40-minutes post injection (mpi), or 1 or 2 hpi).

Laser and filter settings for PMT detectors:
Green channel (GFP): 495-540 nm, 14% laser intensity (488 nm), gain 500.
Red channel (particles, rhodamine B): 560-610 nm, 18-25% laser intensity, gain 750-1050 (higher is for old sphere).
All acquired images are maximum projections of Z-stacks (7.22 µm/slice).

Synthesis of building blocks (SI1)

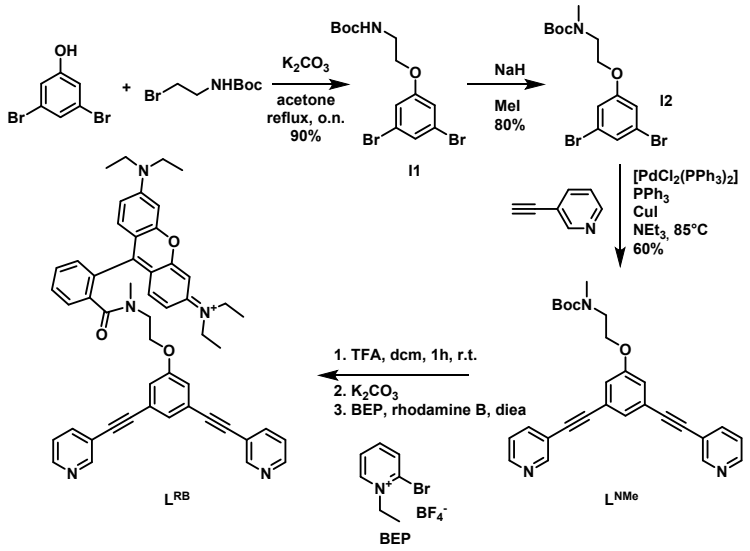

Scheme S1. Synthetic route for the building block L^{RB}.

I1: To a solution of 3,5-dibromo phenol (1 g, 3.98 mmol, 1 eq.) and *tert*-butyl (2-bromoethyl)carbamate (890 mg, 3.98 mmol, 1 eq.) in acetone (100 mL), K_2CO_3 (2.74 g, 19.3 mmol, 5 eq.) was added. The resulting suspension was refluxed overnight. The volatiles were removed under reduced pressure. The crude material was extracted into diethyl ether (100 mL) and washed with $NaHCO_3$, brine and water (50 mL each). The organic layer was dried over $MgSO_4$, filtered and all volatiles were removed under reduced pressure. **I1** was obtained as a white solid (1.4 g, 89%). ^{1}H NMR (400 MHz, Chloroform-*d*) δ 7.29 (d, *J* = 2.1 Hz, 1H), 7.01 (d, *J* = 1.6 Hz, 2H), 4.95 (d, *J* = 10.5 Hz, 1H), 4.01 (t, *J* = 5.1 Hz, 2H), 3.54 (q, *J* = 5.3 Hz, 2H), 1.48 (s, 9H).

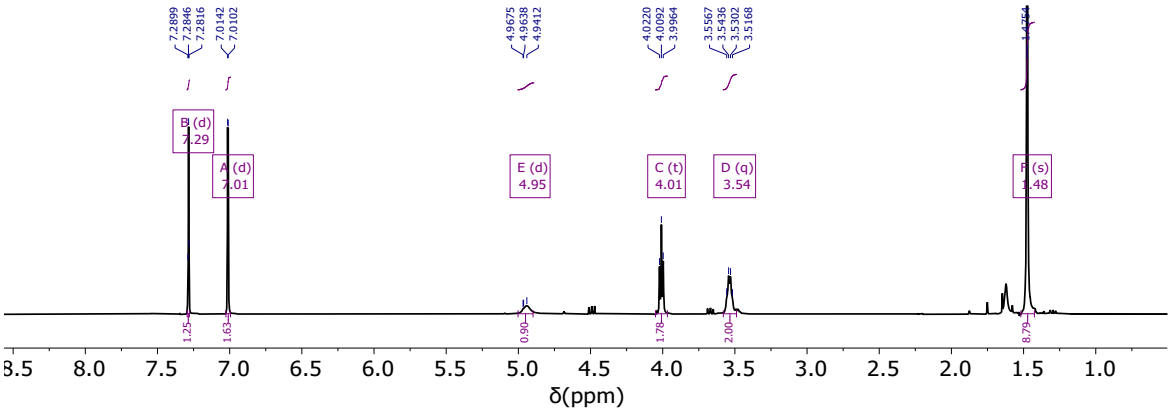

Figure S1. I1 intermediate, ^{1}H NMR in chloroform-*d*.

I2: To a solution of **I1** (1.5 g, 3.85 mmol, 1 eq.) in dry THF (50 mL), MeI (1 mL) was added. Then, NaH (300 mg) were added slowly. The suspension was stirred overnight at room temperature. After quenching the reaction mixture by careful addition of water, the product was extracted with diethyl ether (3 × 50 mL). The organic phase was washed 3 times with brine (3 × 50 mL). The organic phase was dried over $MgSO_4$, filtered and all volatiles were removed under reduced pressure. **I2** was obtained as a colorless oil (1.26 g, 80%). ^{1}H NMR (300 MHz, Chloroform-*d*) δ 7.27 (d, *J* = 1.9 Hz, 1H), 7.00 (d, *J* = 1.7 Hz, 2H), 4.07 (s, 2H), 3.60 (t, *J* = 5.5 Hz, 2H), 2.98 (s, 3H), 1.48 (s, 10H).

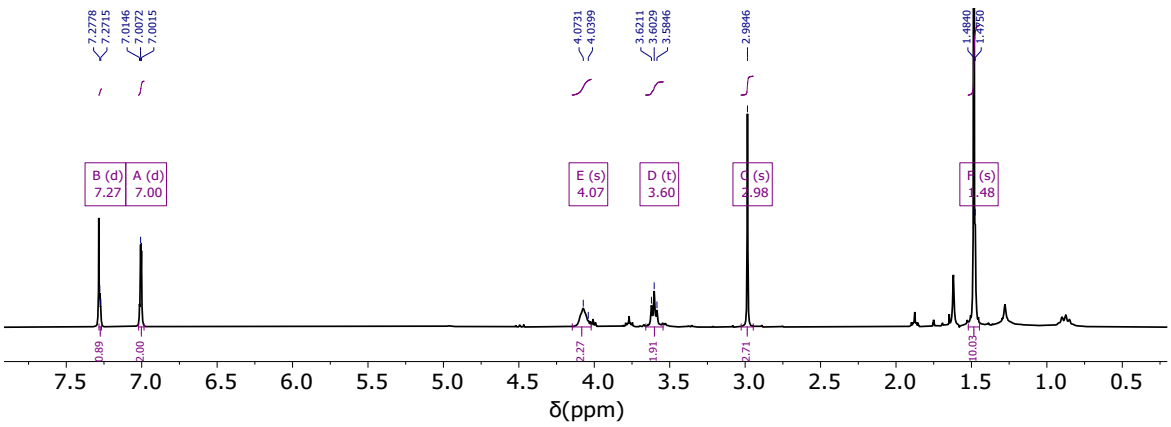

Figure S2. I2 intermediate, ^{1}H NMR in chloroform-*d*.

L^{NMe}: A solution of **I2** (280 mg, 0.7 mmol, 1 eq.) and 3-ethynyl pyridine (180 mg, 1.75 mmol, 2.5 eq.) in triethylamine (10 mL) and dioxane (10 mL) was bubbled with nitrogen for 20 min. Then, [$PdCl_2(PPh_3)_2$] (15 mg, 0.02 mmol, 0.03 eq.) and PPh_3 (11 mg, 0.04 mmol, 0.06 eq.) were added to the solution. The solution was stirred for 20 min before CuI (6 mg, 0.03 mmol, 0.04 eq.) was added. The mixture was heated at 85°C overnight. The volatiles were removed under reduced pressure and the crude material was purified by column chromatography (SiO_2, MeOH:DCM, 1 to 5% MeOH). The product **L^{NMe}** was obtained as an orange oil (190 mg, 57%). ^{1}H NMR (400 MHz, Chloroform-*d*) δ 7.84 (d, *J* = 7.7 Hz, 2H), 7.69 – 7.61 (m, 2H), 7.51 (td, *J* = 7.3, 1.5 Hz, 1H), 7.42 (td, *J* = 7.5, 2.9 Hz, 2H), 7.32 (s, 1H), 7.05 (s, 2H), 4.10 (d, *J* = 8.3 Hz, 2H), 3.71 – 3.54 (m, 2H), 2.96 (s, 3H), 1.45 (s, 8H). ^{13}C NMR (101 MHz, Chloroform-*d*) δ 158.36, 155.76, 155.44, 137.92, 132.93, 132.09, 131.99, 131.95, 131.92, 131.89, 128.54, 128.42, 127.79, 127.64, 123.91, 118.24, 91.81, 91.00, 87.18, 79.74, 70.41, 69.44, 67.14, 66.56, 65.98, 62.97, 53.99, 48.22, 36.25, 35.46, 31.76, 29.66, 29.29, 28.44, 28.39. HR–ESI–MS, calculated for [S-boc+H^{+}] $C_{23}H_{20}N_3O$ 354.1601, obtained 354.1423.

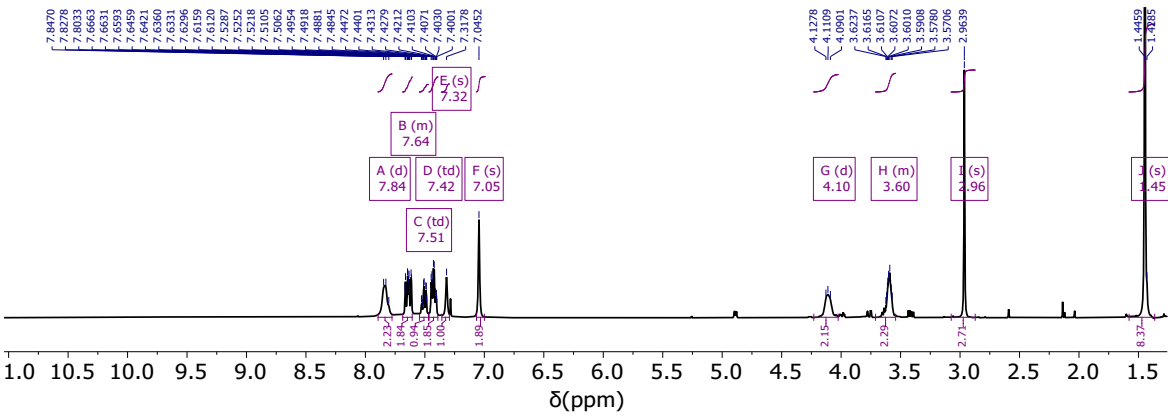

Figure S3. L^{NMe} intermediate, ^{1}H NMR in chloroform-*d*.

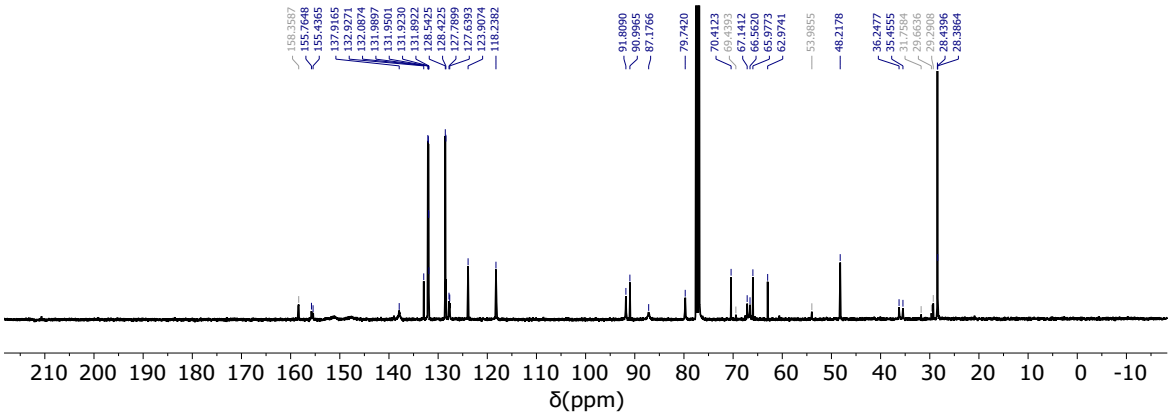

Figure S4. L^{NMe} intermediate, ^{13}C NMR in chloroform-*d*.

L^{RB}: **L^{NMe}** (640 mg, 1.41 mmol) was dissolved in DCM (50 mL). Then, TFA (10 mL) was added. The solution was stirred for 2 h at room temperature. The volatiles were removed under reduced pressure and the crude material was dissolved in a suspension of DCM and $NaHCO_{3aq}$. The organic phase was separated and washed with brine (1 × 50mL). The organic phase was dried over $MgSO_4$, filtered and all volatiles were removed under reduced pressure. The BOC-deprotected material was immediately taken for the next step without any further purification. The intermediate was dissolved in dry DCM (10 mL). Rhodamine B (750 mg, 1.55 mmol, 1.1 eq.) and 2-bromo-1-ethyl pyridinium tetrafluoroborate (BEP, 430 mg, 1.55 mmol, 1.1 eq.) were added. Then, DIPEA (0.8 mL, 4.2 mmol, 3 eq.) was added and the resulting solution was stirred overnight. The product was extracted into DCM and remaining starting material was washed into $NaOH_{aq}$ (1M) (5x 50 mL). The organic solvent was evaporated under reduced pressure. The obtained material was dissolved in MeCN (20 mL) and water (100 mL) containing $NaBF_4$ (10 g) were added. All solvent was evaporated and the product was taken up into MeCN. The organic solvent was evaporated and the crude material was purified by column chromatography (SiO_2, MeOH:DCM, 1 to 15% MeOH). LRB was obtained as a dark red solid (600 mg, 50%). ^{1}H NMR (400 MHz, Acetonitrile-d_3) δ 8.83 (dd, J = 2.2, 0.9 Hz, 2H), 8.64 (dd, J = 4.9, 1.6 Hz, 2H), 7.96 (dt, J = 7.9, 1.9 Hz, 2H), 7.79 – 7.69 (m, 3H), 7.69 – 7.61 (m, 1H), 7.50 – 7.39 (m, 5H), 7.28 (d, J = 9.6 Hz, 2H), 6.95 (dd, J = 9.6, 2.5 Hz, 3H), 6.84 (d, J = 1.4 Hz, 2H), 6.55 (d, J = 2.5 Hz, 2H), 3.66 – 3.45 (m, 12H), 2.90 (s, 3H), 1.19 (t, J = 7.1 Hz, 14H). ^{13}C NMR (101 MHz, acetonitrile-d_3) δ 206.48, 168.49, 158.55, 157.47, 155.50, 155.47, 152.02, 149.33, 138.49, 136.74, 132.21, 130.20, 130.12, 129.97, 129.33, 127.21, 127.11, 123.91, 123.53, 117.31, 113.80, 113.33, 95.72, 91.06, 86.73, 66.75, 54.34, 46.64, 45.65, 38.87, 29.90, 11.83. HR–ESI–MS, calculated for $C_{51}H_{48}N_5O_3$ 778.3752, obtained 778.3156.

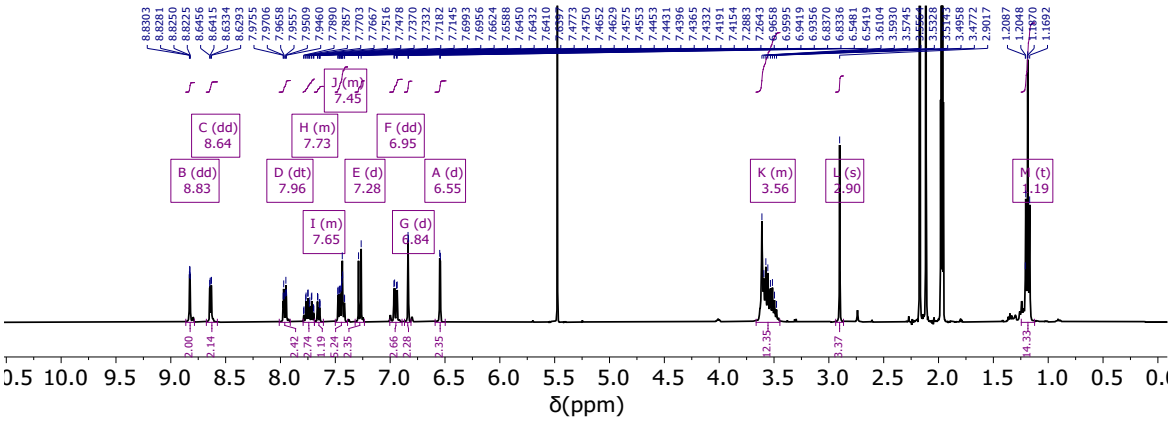

Figure S5. L^{RB} building block, ^{1}H NMR in acetonitrile-d_3.

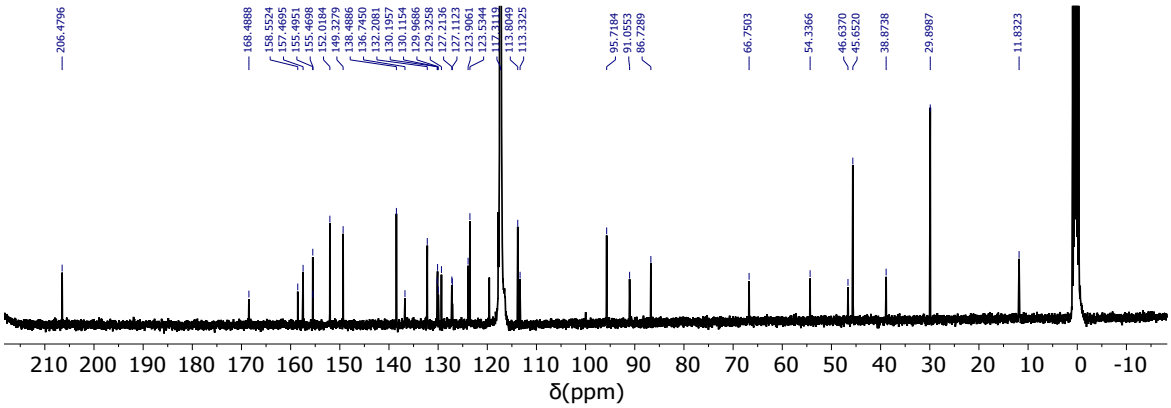

Figure S6. L^{RB} building block, ^{13}C NMR in acetonitrile-d_3.

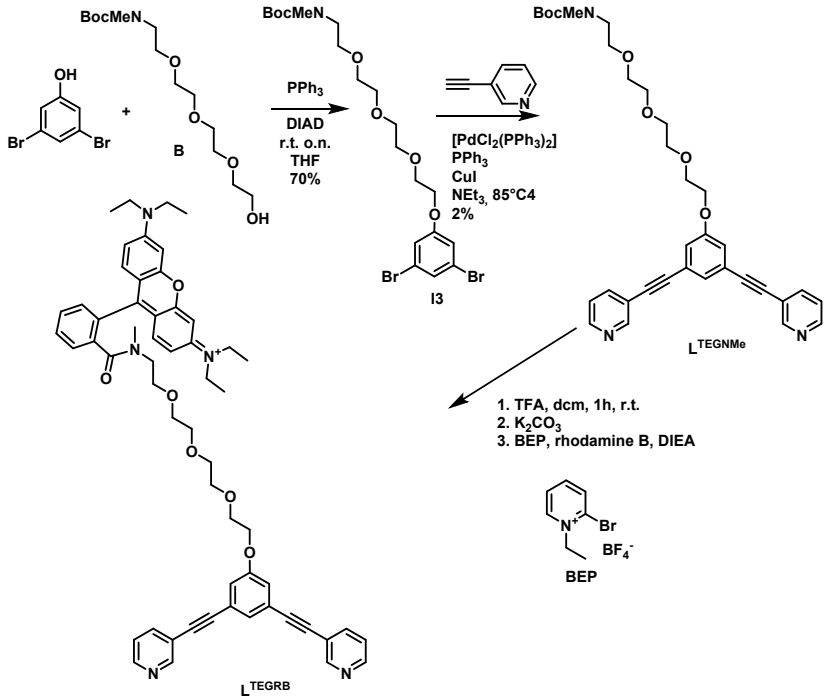

Scheme S2. Synthetic route for the building block L^{TEGRB}.

I3: To a solution of 3,5-dibromo phenol (3 g, 11.9 mmol, 1 eq.), **B** (3.6 g, 11.9 mmol, 1 eq.) and PPh3 (3.2 g, 11.9 mmol, 1 eq.) in dry THF (30 mL), DIAD (2.64 g, 13 mmol, 1.1 eq.) was slowly added. The resulting solution was stirred overnight. All volatiles were evaporated under reduced pressure. The crude material was purified by column chromatography (SiO_2, EtOAc:heptane, 10 to 50% EtOAc). **I3** was obtained as a colorless oil (4.5 g, 70%). ^{1}H NMR (300 MHz, Chloroform-*d*) δ 7.27 (t, *J* = 1.6 Hz, 1H), 7.04 (d, *J* = 1.7 Hz, 2H), 5.00 (p, *J* = 6.3 Hz, 1H), 4.22 – 4.05 (m, 2H), 3.90 – 3.81 (m, 2H), 3.71 (ttd, *J* = 5.7, 2.9, 1.1 Hz, 4H), 3.64 (hept, *J* = 2.7 Hz, 3H), 3.41 (s, 3H), 2.93 (s, 4H), 1.47 (s, 11H).

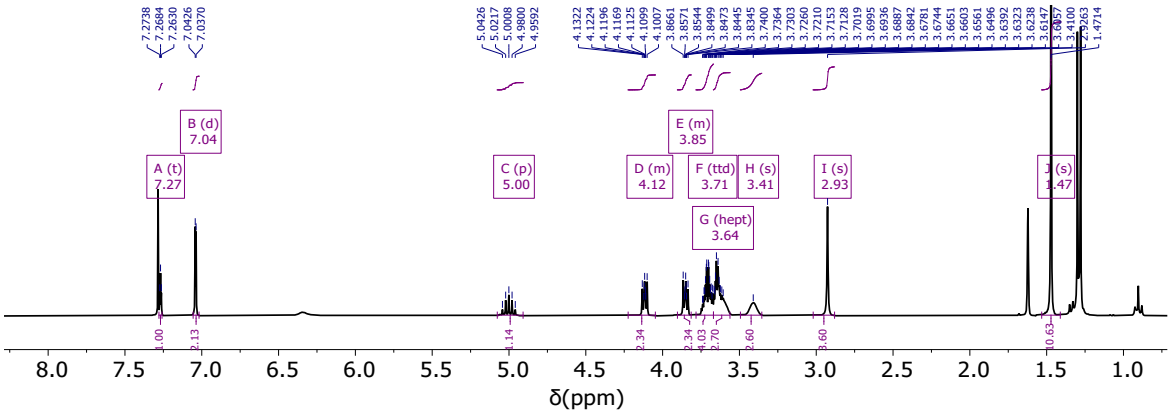

Figure S7. I3 intermediate, ^{1}H NMR in chloroform-*d*.

L^{TEGNMe}: To a solution of **I3** (2 g, 3.7 mmol, 1 eq.) and 3-ethynylpyridine (1 g, 9.42 mmol, 2.5 eq.) in triethylamine (20 mL) and dioxane (20 mL), [$PdCl_2(PPh_3)_2$] (100 mg, 0.03 eq.) and PPh_3 (60 mg, 0.06 eq.) were added to the solution. The solution was stirred for 20 min before CuI (30 mg, 0.04 eq.) was added. The mixture was heated at 85°C for 3 days. The volatiles were removed under reduced pressure and the crude material was purified by column chromatography (SiO_2, $CHCl_3$:acetone, 3:1). The product **L^{TEGNMe}** was obtained as an colorless oil (900 mg).H NMR (300 MHz, Chloroform-*d*) δ 8.80 – 8.73 (m, 2H), 8.56 (dd, *J* = 4.9, 1.7 Hz, 2H), 7.80 (dt, *J* = 7.9, 1.9 Hz, 2H), 7.34 (t, *J* = 1.4 Hz, 1H), 7.09 (d, *J* = 1.4 Hz, 2H), 4.17 (dd, *J* = 5.7, 3.9 Hz, 2H), 3.91 – 3.83 (m, 2H), 3.76 – 3.67 (m, 4H), 3.67 – 3.53 (m, 3H), 3.38 (s, 3H), 2.89 (s, 4H), 1.44 (s, 11H).

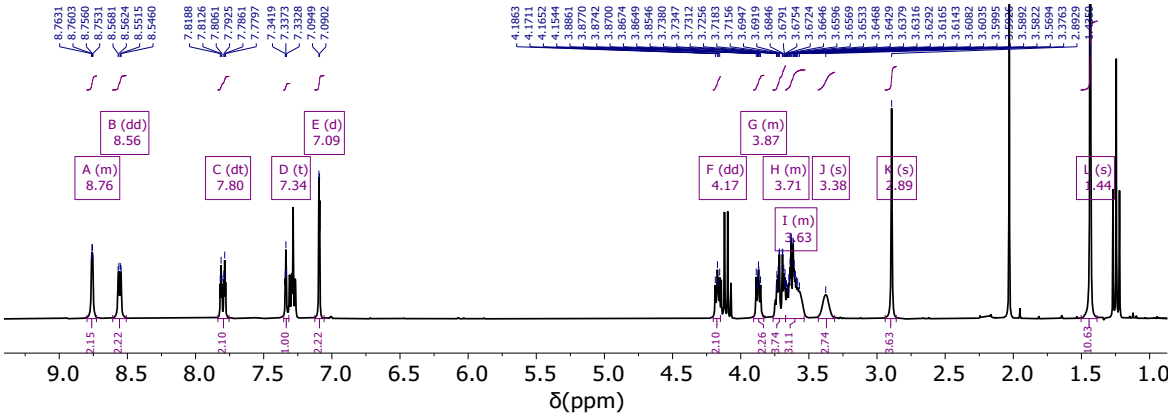

Figure S8. L^{TEGNMe} intermediate, ^{1}H NMR in chloroform-d.

L^{TEGRB}: **L^{TEGNMe}** (500 mg, 0.85 mmol) was dissolved in 50 mL DCM. Then, 3 mL TFA was added. The solution was stirred for 2 h at room temperature. The volatiles were removed under reduced pressure and the crude material was dissolved in a suspension of DCM and $NaHCO_{3aq}$. The organic phase was separated and washed with brine (1x50mL). The organic phase was dried over $MgSO_4$, filtered and all volatiles were removed under reduced pressure. The boc-deprotected material was immediately taken for the next step without any further purification. The intermediate was dissolved in 10 mL dry DCM. Rhodamine B (450 mg, 0.94 mmol, 1.1 eq.) and 2-Bromo-1-ethyl Pyridinium Tetrafluoroborate (BEP) (260 mg, 0.94 mmol, 1.1 eq.) were added. Then, DIPEA (0.5 mL, 2.56 mmol, 3 eq.) was added and the resulting solution was stirred overnight. The product was extracted into DCM and remaining starting material was washed into $NaOH_{aq}$ (1M) (5x 100 mL). The organic solvent was evaporated under reduced pressure. The obtained material was dissolved in 20 mL MeCN and 100 mL water containing 10g $NaBF_4$ were added. All solvent was evaporated and the product was taken up into MeCN. The organic solvent was evaporated and the crude material was purified by column chromatography (SiO_2, MeOH:DCM, 1 to 15% MeOH). **L^{TEGRB}** was obtained as a dark red solid (250 mg). ^{13}C NMR (75 MHz, $CDCl_3$) δ 168.38, 158.60, 157.70, 156.08, 155.58, 152.09, 148.78, 138.64, 136.28, 132.06, 130.45, 130.07, 129.97, 129.82, 129.53, 129.26, 128.84, 127.59, 127.46, 123.86, 123.24, 120.02, 118.33, 113.96, 113.64, 99.99, 96.19, 96.12, 91.53, 86.49, 70.80, 70.56, 70.44, 70.16, 69.51, 68.68, 67.88, 53.53, 47.09, 46.00, 39.15, 32.19, 12.58. ^{1}H NMR (300 MHz, Acetonitrile-d_3) δ 8.74 (d, *J* = 2.1 Hz, 2H), 8.60 (dd, *J* = 4.9, 1.7 Hz, 2H), 7.89 (dt, *J* = 7.9, 2.0 Hz, 2H), 7.71 (dd, *J* = 6.3, 3.5 Hz, 2H), 7.47 – 7.39 (m, 2H), 7.36 (d, *J* = 10.4 Hz, 1H), 7.22 (d, *J* = 9.5 Hz, 2H), 7.15 (d, *J* = 1.3 Hz, 2H), 6.97 (dd, *J* = 9.5, 2.5 Hz, 2H), 6.81 (s, 2H), 4.18 (t, *J* = 4.5 Hz, 2H), 3.89 – 3.76 (m, 2H), 3.64 (q, *J* = 7.2 Hz, 11H), 3.47 (q, *J* = 7.0 Hz, 1H), 3.34 (t, *J* = 5.4 Hz, 2H), 2.13 (s, 7H), 1.29 (t, *J* = 7.1 Hz, 12H). HR-ESI-MS, calculated for $C_{57}H_{60}N_5O_6$ 910.4539, obtained 910.4253.

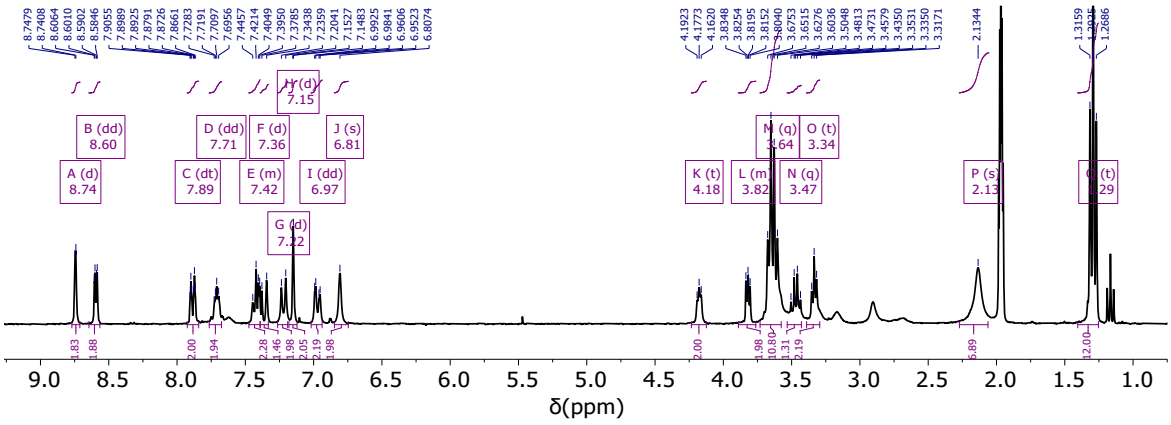

Figure S9. L^{TEGRB} building block, ^{1}H NMR in acetonitrile-d_3.

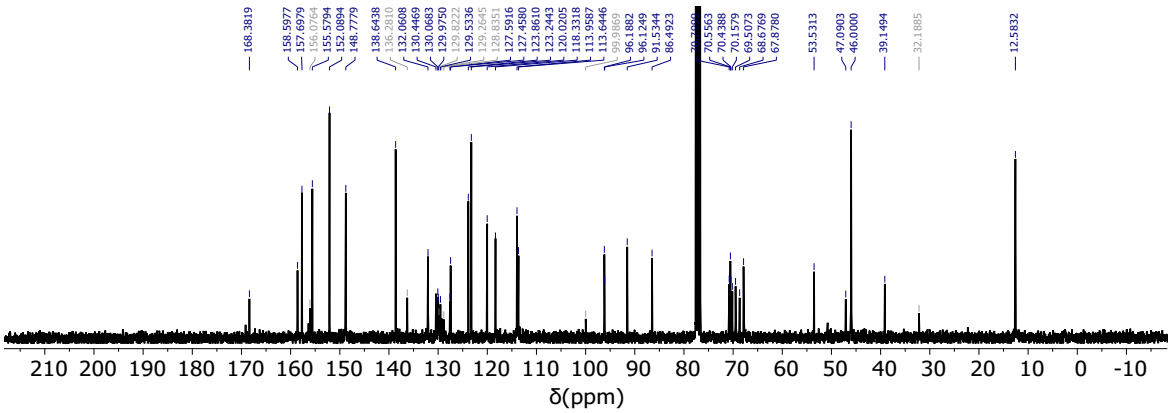

Figure S10. L^{TEGRB} building block, ^{13}C NMR in acetonitrile-d_3.

Nanosphere Synthesis (SI2)

$Pt_2L^{RB}_4$

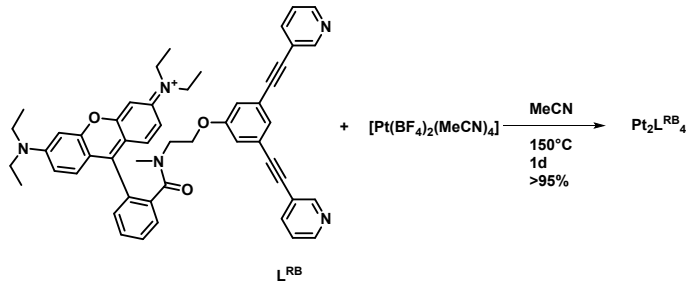

Scheme S3. Synthesis of the $Pt_2L^{RB}_4$ sphere.

A solution of $\mathbf{L^{RB}}$ (8.65 mg, 10 μmol, 1 eq.) and $[Pt(BF_4)_2(MeCN)_4]$ (3.2 mg, 6 μmol, 0.6 eq.) was heated at 150°C for 1d. The sphere was precipitated in diethyl ether and redissolved in DMSO for further studies. ^{1}H NMR (300 MHz, Deuterium Oxide) δ 10.10 (s, 2H), 9.70 (d, *J* = 6.0 Hz, 2H), 8.39 (d, *J* = 8.2 Hz, 2H), 8.02 (q, *J* = 6.4 Hz, 4H), 7.91 (dd, *J* = 29.2, 7.6 Hz, 1H), 7.51 (dd, *J* = 21.5, 8.6 Hz, 2H), 7.15 (d, *J* = 10.1 Hz, 3H), 6.47 (s, 1H), 3.85 – 3.47 (m, 13H), 2.97 (s, 2H), 1.29 (d, *J* = 35.2 Hz, 14H).

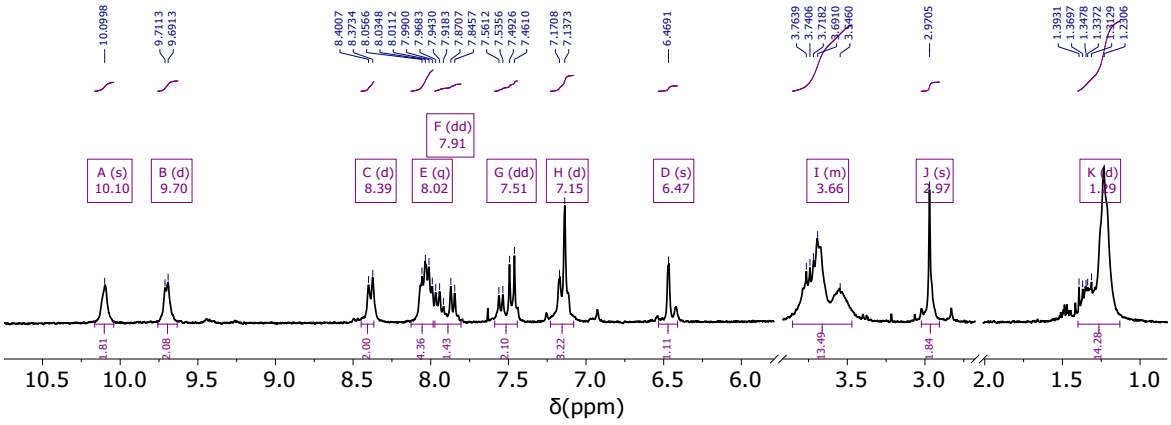

Figure S11. $Pt_2L^{RB}_4$ sphere, ^{1}H NMR in acetonitrile-d_3+D_2O.

$Pt_2L^{TEGRB}{}_4$

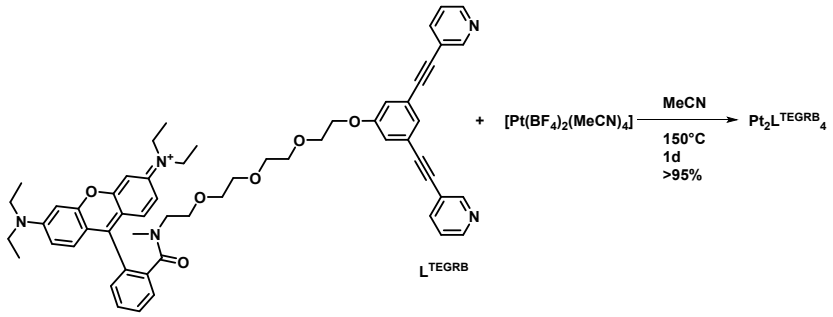

Scheme S4. Synthesis of the $Pt_2L^{TEGRB}{}_4$ sphere.

A solution of $\mathbf{L}^{TEGRB}$ (9.97 mg, 10 µmol, 1 eq.) and $[Pt(BF_4)_2(MeCN)_4]$ (3.2 mg, 6 µmol, 0.6 eq.) was heated at 150°C for 1d. The sphere was precipitated in diethyl ether and redissolved in DMSO for further studies. ^{1}H NMR (300 MHz, DMSO-d_6) δ 9.46 – 9.27 (m, 4H), 8.20 (d, *J* = 8.0 Hz, 2H), 7.91 – 7.78 (m, 2H), 7.72 (dd, *J* = 8.8, 4.7 Hz, 2H), 7.64 – 7.54 (m, 1H), 7.50 (t, *J* = 4.5 Hz, 1H), 7.28 (s, 2H), 7.18 – 7.01 (m, 4H), 6.91 (d, *J* = 2.1 Hz, 2H), 4.11 (s, 2H), 3.78 – 3.42 (m, 15H), 3.27 – 3.14 (m, 2H), 2.91 (d, *J* = 30.8 Hz, 3H), 1.18 (t, *J* = 7.0 Hz, 15H).

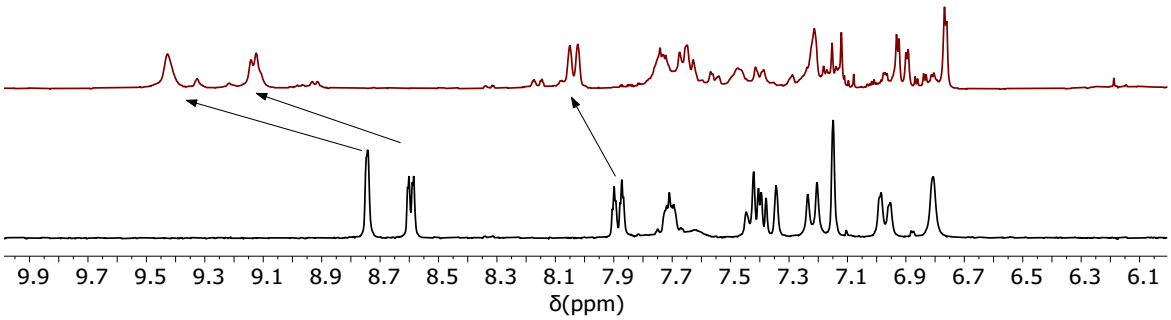

Figure S12. $Pt_2L^{TEGRB}{}_4$ sphere (top) and corresponding building block (bottom), ^{1}H NMR in acetonitrile-d_3.

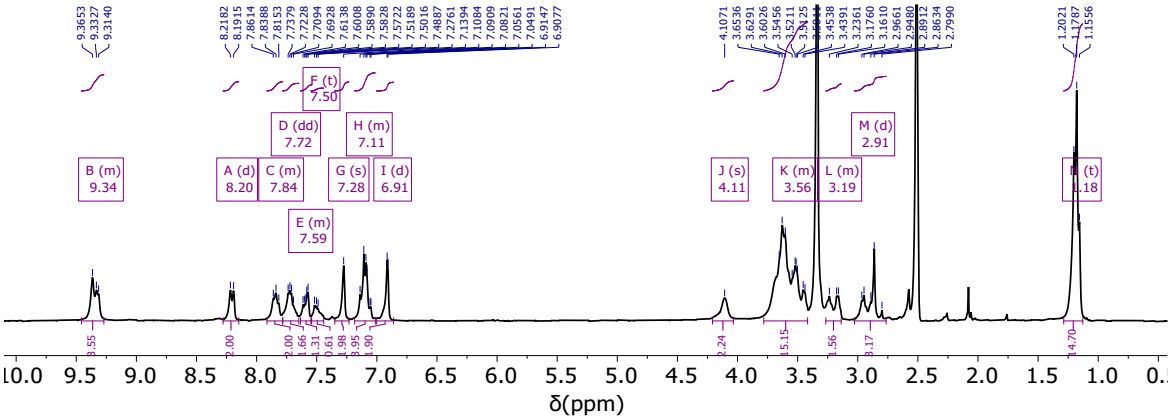

Figure S13. $Pt_2L^{TEGRB}{}_4$ sphere, ^{1}H NMR in DMSO-d_6.

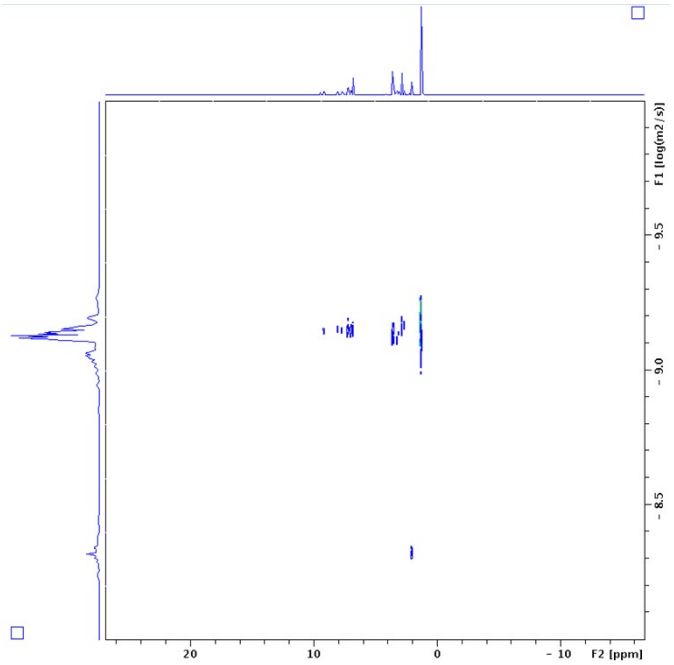

Figure S14. $Pt_2L^{TEGRB}{}_4$ sphere, DOSY H NMR in MeCN-d_3.

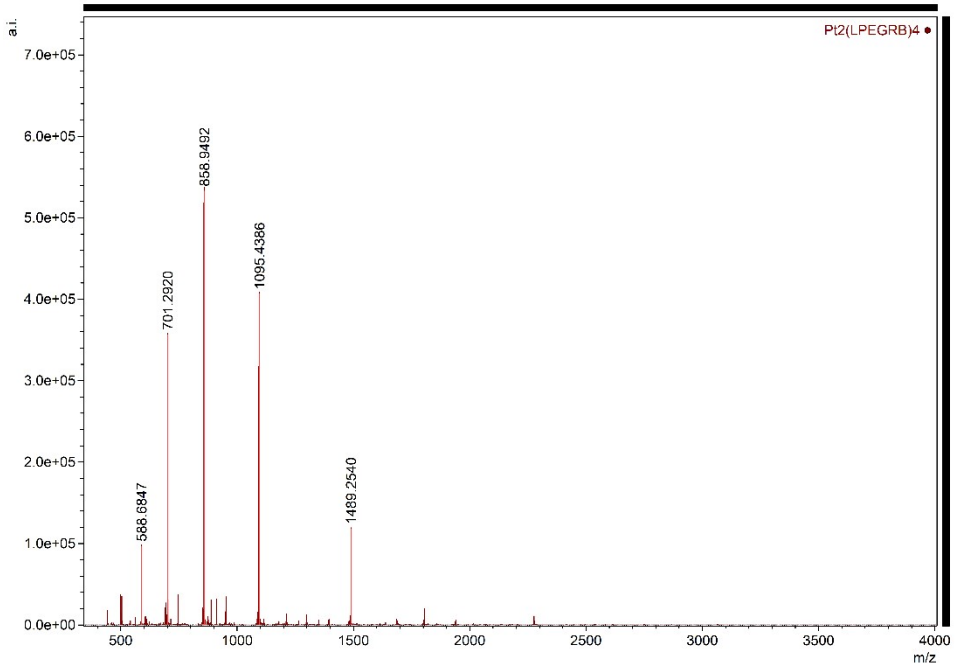

Figure S15. ESI-MS spectra of $Pt_2L^{TEGRB}{}_4$ sphere, showing signals corresponding to the 3-7$^+$ species.

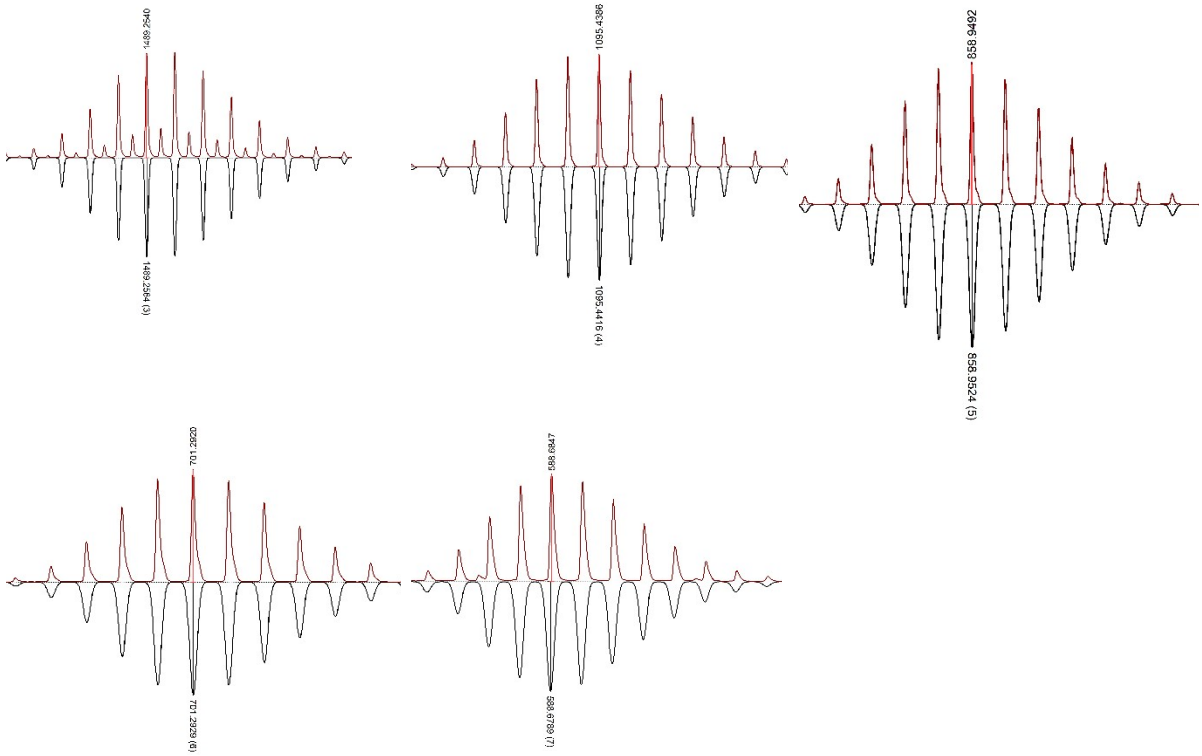

Sphere Stability (SI3)

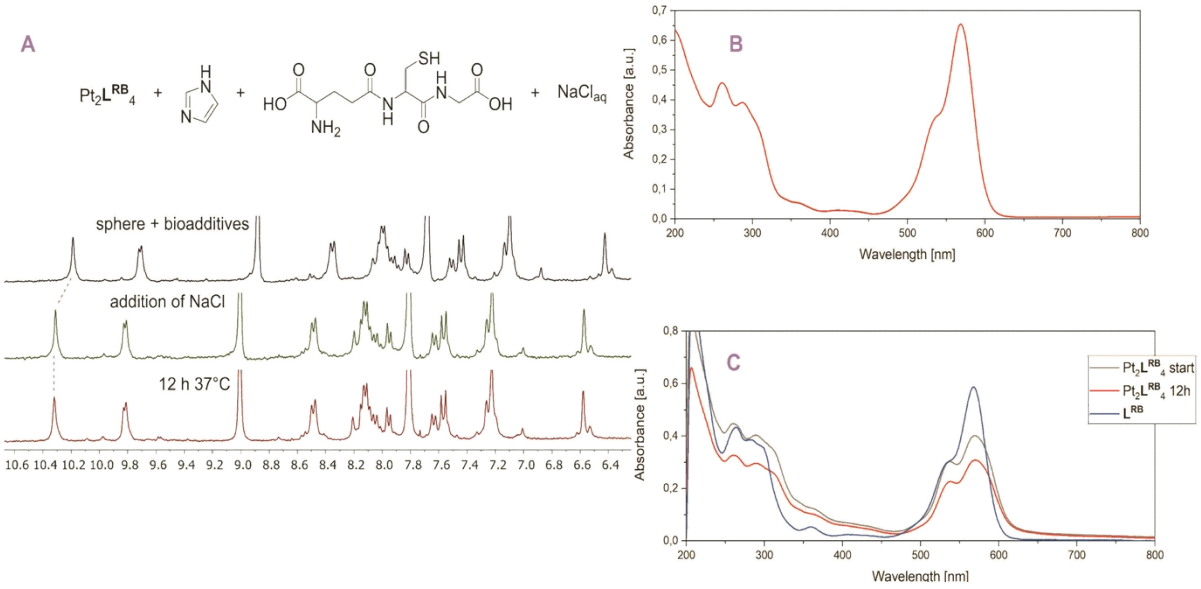

Figure S16. Chemical stability of $Pt_2L^{RB}_4$ in the presence of nucleophiles and reducing agents studied by ^{1}H-NMR (A). UV/Vis absorption of $Pt_2L^{TEGRB}_4$ in PBS (1M, pH 7.4) measured directly and after 12 h at 37°C (B). UV/Vis absorption of $Pt_2L^{RB}_4$ in PBS (1M, pH 7.4) measured directly and after 12 h at 37°C (C).

***In vitro* cytotoxicity data (SI4)**

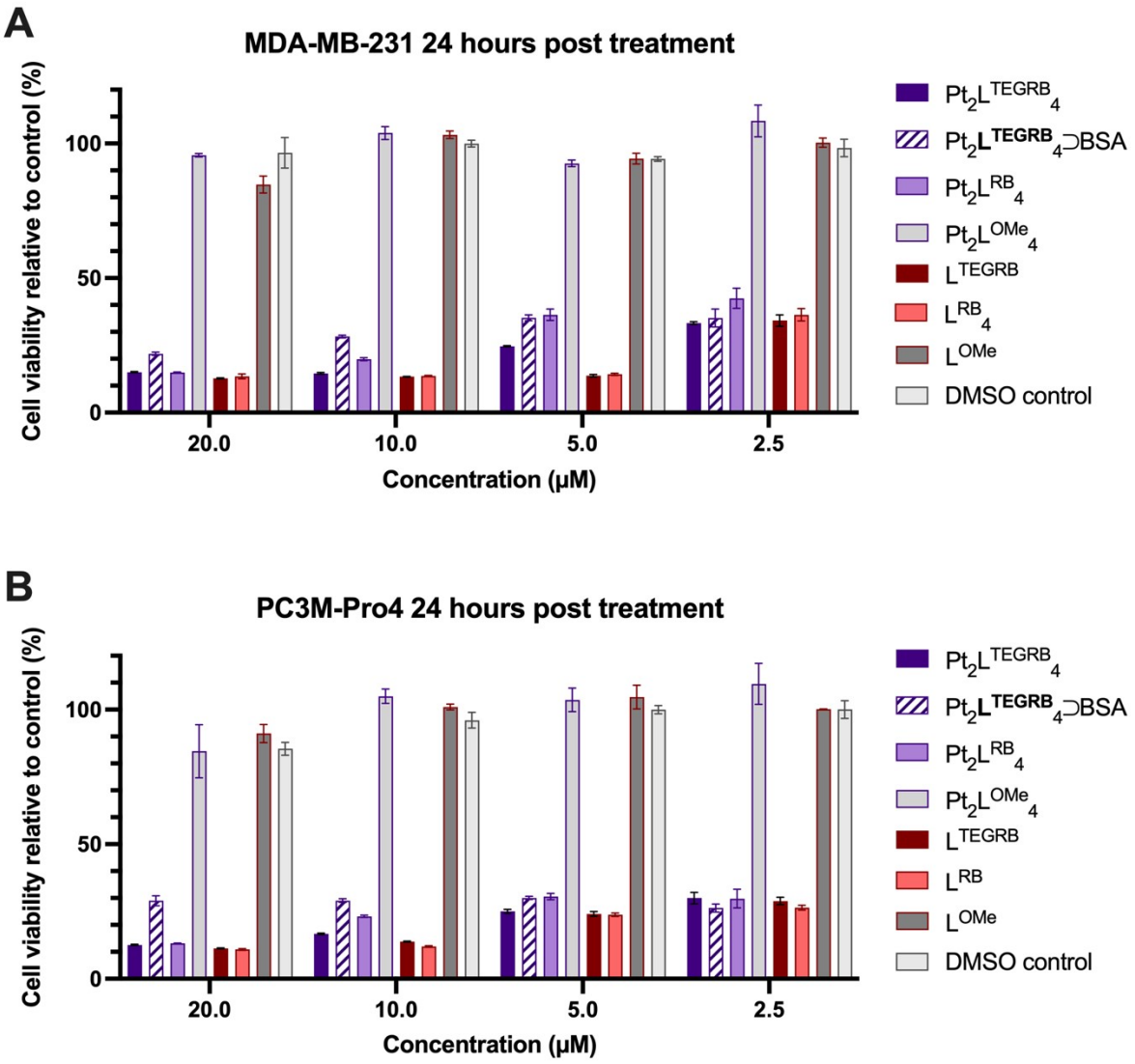

Figure S17. ***In vitro*** **cytotoxicity analysis by cell viability assay using WST-1 reagent in two cancer cell lines. Concentrations of various sphere materials ranging from 2.5 to 20 μM in (A) MDA-MB-231 breast cancer cell line and (B) PC3M-Pro4 prostate cancer cell line.**

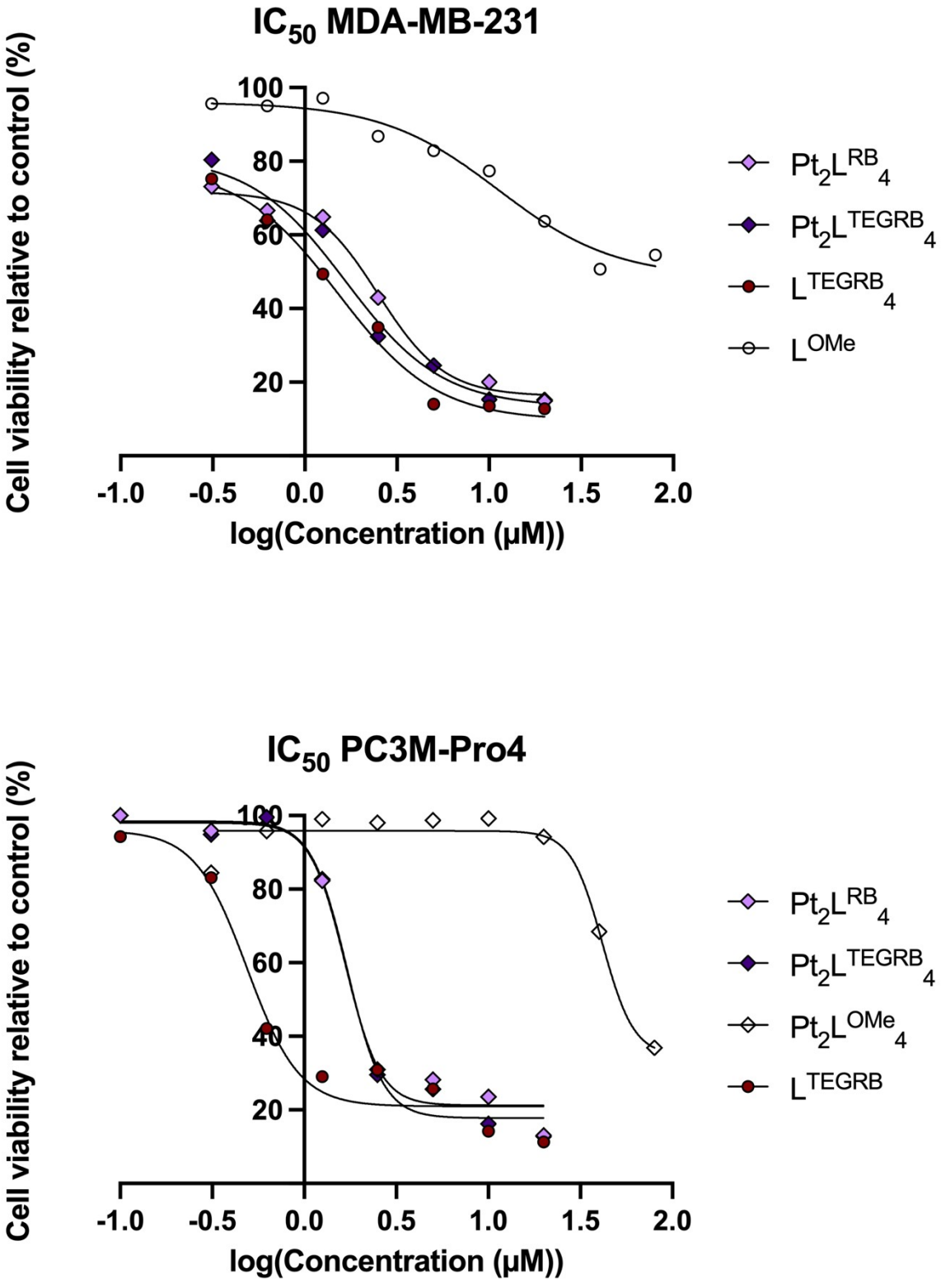

Figure S18. ***In vitro*** **cytotoxicity analysis by cell viability assay using WST-1 reagent in two cancer cell lines. Concentrations of various sphere materials against MDA-MB-231 (top) breast cancer cell line and PC3M-Pro4 prostate cancer cell line (bottom) for determination of IC_{50}.**

ITC supplementary data (SI5)

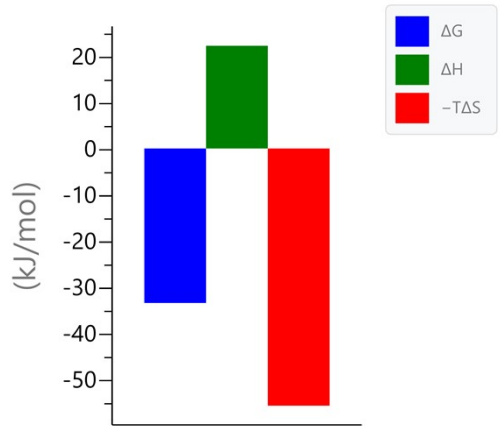

Figure S19. "Signature plot" of $Pt_2L^{RB}_4$ (right) and $Pt_2L^{TEGRB}_4$ (left).

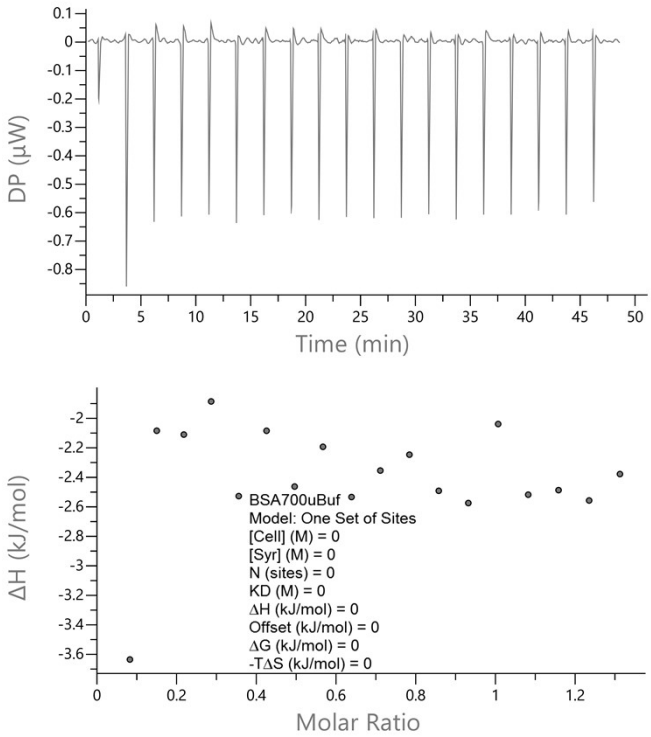

Figure S20. Control titration of BSA to buffer.

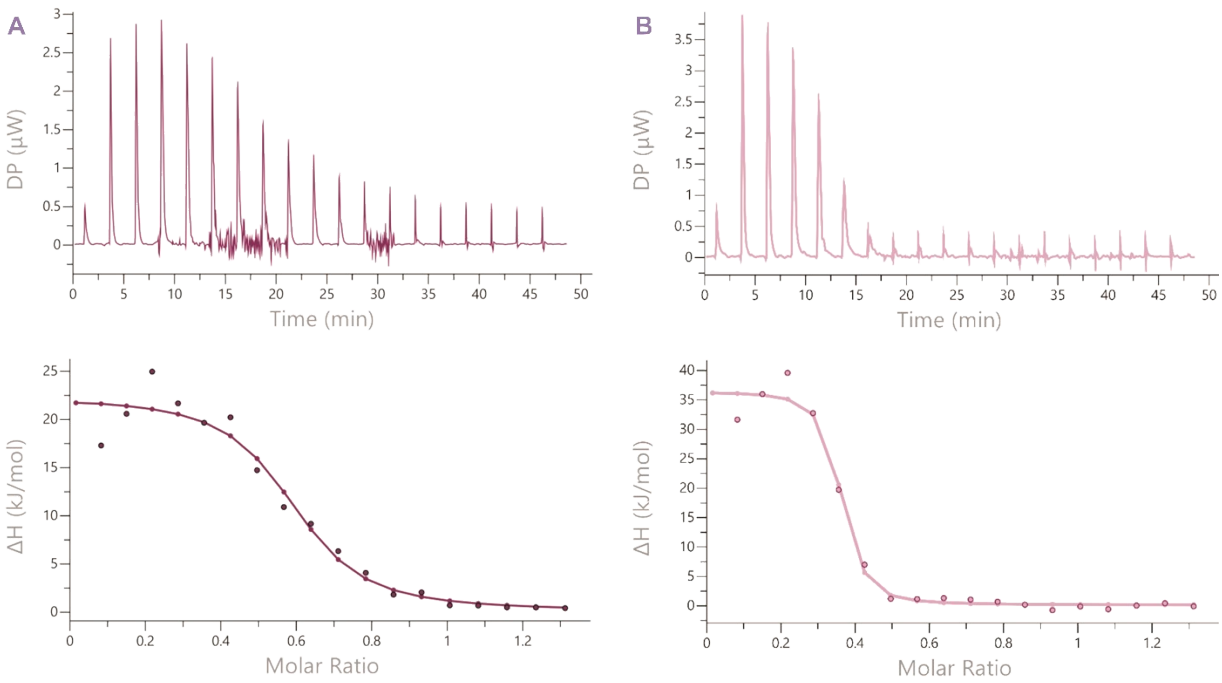

Figure S21. ITC titrations for the addition of BSA to $Pt_2L^{TEGRB}{}_4$ (A) and $Pt_2L^{RB}{}_4$ (B). Above: ITC thermograms and below: fitted binding isotherms to obtain the corresponding thermodynamic parameters.

Biodistribution supplementary data (SI6)

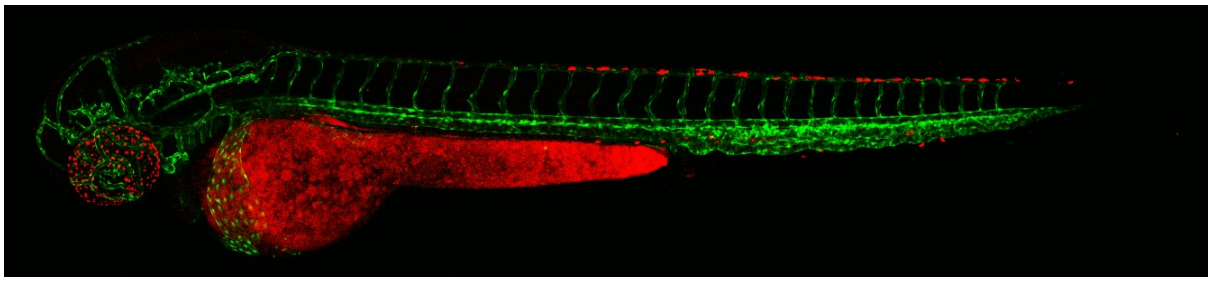

Figure S22. Non-injected 54 hpf transgenic *kdrl*:EGFP zebrafish embryo showing red autofluorescence at microscope settings used for imaging of low concentration samples (5 µM).

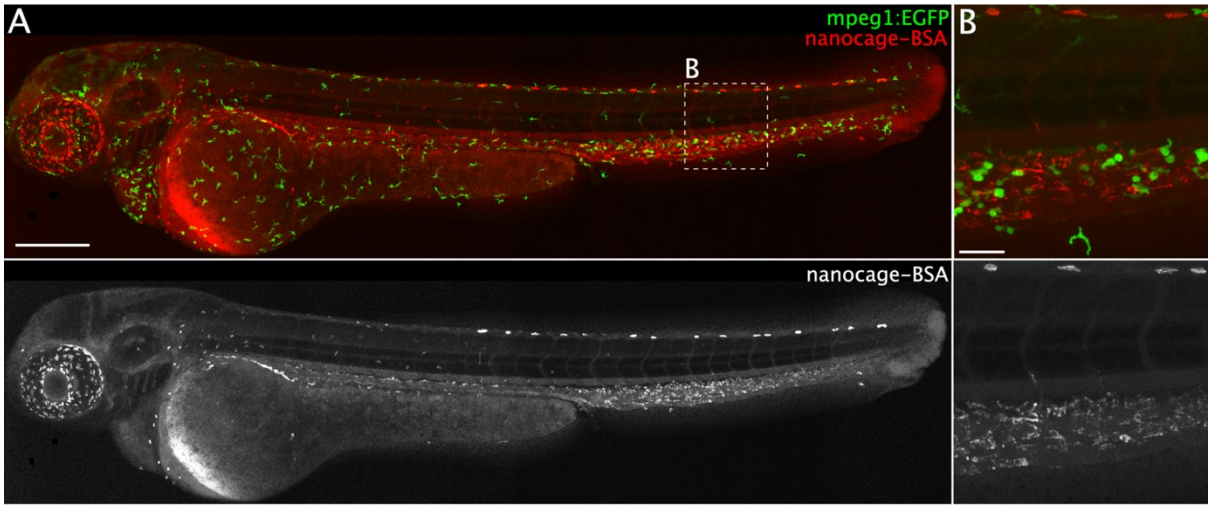

Figure S23. Confocal images showing biodistribution of 5 µM $Pt_2L^{RB}_4$⊃BSA **intravenously injected (1 nl) in 54 hpf transgenic *mpeg1*:EGFP zebrafish embryos. (A)** Whole embryo and **(B)** tissue level (scavenger endothelial cells, SECs) views of nanoparticle biodistribution. No macrophage uptake was observed over the course of 1.5 hours as depicted by lack of fluorescence overlap. SEC uptake was observed as well as accumulation in ionocytes and slight accumulation in the pronephric duct (schematically depicted in figure S25). Scale bars represent 250 µm (A) and 50 µm (B).

Computational modeling (SI7)

A model of the $Pt_2L^{RB}_4$ sphere was constructed following our previously reported methodology[2]. These models were successively docked with PLANTS1.2 [3] into prepared protein structures of BSA obtained from x-ray crystallography data (RCSB ID: 3V03, 4F5S, 4JK4, 4OR0, 5OSW, 6QS9). The pose with the best ChemPLP dock score was then used for docking of a second $Pt_2L^{RB}_4$ sphere with the same parameters. The resulting best pose for two docked spheres was then solvated with TIP3P water and neutralised by addition of chloride anions following standard procedures. The resulting coordinates and parameter-topology files were then used in amber[4-5] for a short molecular dynamics (20 ns, T = 300 K) following standard protocol including heating (1 ns), equilibration (5 ns) and productive (20 ns) phases to relax the docked configuration. The final structure was used as the representative of the BSA-$Pt_2L^{RB}_4$ complex.

Single-Crystal X-Ray Diffraction data (SI8) of the $Pt_2L^{RB}_4$ sphere (SI8)

X-ray diffraction data of **$Pt_2L^{RB}_4$** were measured on a Bruker D8 Quest Eco diffractometer using graphite-monochromated (Triumph) Mo Ka radiation (λ = 0.71073 Å) and a CPAD Photon III C14 detector. The sample was cooled with N_2 to 100 K with a Cryostream 700 (Oxford Cryosystems). Intensity data were integrated using the SAINT software.[6] Absorption correction and scaling was executed with SADABS.[7] The structures were solved using intrinsic phasing with the program SHELXT 2018/2.[8] The crystal structure contained two voids (total solvent accessible volume = 1673 Å^3), and the highly disordered, anion and solvent molecules (BF_4^-, Et_2O and CH_3CN) within the asymmetric unit could not be refined reliably. Thus, the SQUEEZE[9] procedure in PLATON[10] (version 100822) was applied, accounting for 911 electrons per unit cell, congruent with the presence of 4 × BF_4^- (40 e^-/molecule), 5 × Et_2O (37 e^-/molecule) and 5 × CH_3CN (22 e^-/molecule) molecules in the unit cell (912 e^- total). Least-squares refinement was performed with SHELXL-2018/3.[11] All non-hydrogen atoms were refined with anisotropic displacement parameters. The hydrogen atoms were introduced at calculated positions with a riding model. The X-ray crystallographic data for **$Pt_2L^{RB}_4$** was deposited at the Cambridge Crystallographic Data Centre (CCDC), under the deposition number CCDC 2216167.

$Pt_2L^{RB}_4$: $C_{204}H_{192}N_{20}O_{12}Pt_2^{4+}$, 4$(BF_4)^-$, 5$(C_4H_{10}O)$, 5$(C_2H_3N)$, Fw = 4403.85, block, 0.210 × 0.166 × 0.140, triclinic, P-1, (No: 2), a = 17.6863(14), b = 18.9328(15), c = 20.2709(17) Å, α = 114.660(4), β = 97.896(4), γ = 108.962(3)°, V = 5531.9(8) Å^3, Z = 1, D_x = 1.322 g cm^{-3}, µ = 1.344 mm^{-1}. 335633 Reflections were measured up to a resolution of (sinθ/λ)max = 0.84 Å^{-1}. 19472 Reflections were unique (R_{int} = 0.1881), of which 11573 were observed [$I > 2\sigma(I)$]. 1082 Parameters were refined with 1017 restraints. R_1/wR_2 [$I > 2\sigma(I)$]: 0.1262/0.2622. R_1/wR_2 [all refl.]: 0.2012/0.3166. S = 1.121. Residual electron density between -1.921 and 2.271 e^- Å^{-3}. CCDC 2216167

References (SI9)

[1] Sepehrpour, H.; Fu, W.; Sun, Y.; Stang, P. J. Biomedically Relevant Self-Assembled Metallacycles and Metallaspheres. *J. Am. Chem. Soc.*, **2019**, *141*, 14005–14020. https://doi.org/10.1021/jacs.9b06222.

[2] Poole, D. A.; Bobylev, E. O.; Mathew, S.; Reek, J. N. H. Topological Prediction of Palladium Coordination Spheres. *Chem. Sci.*, **2020**, *11*, 12350–12357. https://doi.org/10.1039/d0sc03992f.

[3] Korb, O.; Stützle, T.; Exner, T. E. Empirical Scoring Functions for Advanced Protein−Ligand Docking with PLANTS. *J. Chem. Inform. Model.*, **2009**, *49*, 84–96. https://doi.org/10.1021/ci800298z.

[4] D.A. Case, H.M. Aktulga, K. Belfon, I.Y. Ben-Shalom, J.T. Berryman, S.R. Brozell, D.S. Cerutti, T.E. Cheatham, III, G.A. Cisneros, V.W.D. Cruzeiro, T.A. Darden, R.E. Duke, G. Giambasu, M.K. Gilson, H. Gohlke, A.W. Goetz, R. Harris, S. Izadi, S.A. Izmailov, K. Kasavajhala, M.C. Kaymak, E. King, A. Kovalenko, T. Kurtzman, T.S. Lee, S. LeGrand, P. Li, C. Lin, J. Liu, T. Luchko, R. Luo, M. Machado, V. Man, M. Manathunga, K.M. Merz, Y. Miao, O. Mikhailovskii, G. Monard, H. Nguyen, K.A. O'Hearn, A. Onufriev, F. Pan, S. Pantano, R. Qi, A. Rahnamoun, D.R. Roe, A. Roitberg, C. Sagui, S. Schott-Verdugo, A. Shajan, J. Shen, C.L. Simmerling, N.R. Skrynnikov, J. Smith, J. Swails, R.C. Walker, J. Wang, J. Wang, H. Wei, R.M. Wolf, X. Wu, Y. Xiong, Y. Xue, D.M. York, S. Zhao, and P.A. Kollman (2022), Amber 2022, University of California, San Francisco. https://ambermd.org/CiteAmber.php

[5] see Amber manual 20, https://www.google.com/url?sa=t&source=web&rct=j&url=https://ambermd.org/doc12/Amber21.pdf&ved=2ahUKEwjNjebzz5H7AhWBHewKHQNLDTMQFnoECBoQAQ&usg=AOvVaw27GAnDdoZd-vyZfXREZwOP

[6] Bruker, SAINT V8.40B, Bruker AXS Inc., Madison, Wisconsin, USA, 2001.

[7] SADABS-2016/2 - Bruker AXS area detector scaling and absorption correction: Krause, L., Herbst-Irmer, R., Sheldrick G.M. & Stalke D., *J. Appl. Cryst.*, **2015**, *48*, 3-10. https://doi.org/10.1107/S1600576714022985

[8] Sheldrick, G.M. SHELXT—Integrated space-group and crystal-structure determination. *Acta Crystallogr. Sect. A* **2015**, *A71*, 3–8. https://doi.org/10.1107/S2053273314026370

[9] SQUEEZE - Spek, A. L. PLATON SQUEEZE: a tool for the calculation of the disordered solvent contribution to the calculated structure factors. *Acta Crystallogr.* **2015**, *C71*, 9−18. https://doi.org/10.1107/S2053229614024929

[10] Spek, A. L. (2001). PLATON. Utrecht University, The Netherlands. http://www.Cryst.Chem.uu.nl.

[11] Sheldrick, G.M. Crystal structure refinement with SHELXL. *Acta Crystallogr. Sect. C Struct. Chem.* **2015**, *C71*, 3–8. https://doi.org/10.1107/S2053229614024218